

On 60 GHz Wireless Link Performance in Indoor Environments

Xiaozheng Tie^{1*}, Kishore Ramachandran², and Rajesh Mahindra²

¹ University of Massachusetts, Amherst, MA.

² NEC Laboratories America, Princeton, NJ.

Abstract

The multi-Gbps throughput potential of 60 GHz wireless interfaces make them an attractive technology for next-generation gigabit WLANs. For increased coverage, and improved resilience to human-body blockage, beamsteering with high-gain directional antennas is emerging to be an integral part of 60 GHz radios. However, the real-world performance of these state-of-the-art radios in typical indoor environments has not previously been explored well in open literature.

To this end, in this paper, we address the following open questions: how do these radios perform in indoor line-of-sight(LOS) and non-line-of-sight (NLOS) locations? how sensitive is performance to factors such as node orientation or placement? how robust is performance to human-body blockage and mobility? Our measurement results from a real office setting, using a first-of-its-kind experimental platform (called Presto), show that, contrary to conventional perception, state-of-the-art 60 GHz radios perform well even in NLOS locations, in the presence of human-body blockage and LOS mobility. While their performance is affected by node (or more precisely, antenna array) orientation, simply using a few more antenna arrays and dynamically selecting amongst them shows potential to address this issue. The implications of these observations is in lowering the barriers to their adoption in next-generation gigabit WLANs.

1 Introduction

Emerging radios in the unlicensed 57-66 GHz spectrum (colloquially known as “60 GHz” radios) [23, 6, 22, 9, 1] offer the opportunity to enable throughput-intensive, short-range wireless networks (e.g. [8]) and new services (such as sync-and-go file transfers). By leveraging a wide channel bandwidth (~ 2 GHz), these radios can support over-the-air multi-Gbps data transfers. A caveat, however, is that 60 GHz radios need high-gain directional communication to leverage their throughput potential at distances greater than a few meters [4]. In addition, signals at these millimeter-wavelength frequencies are blocked by human bodies [3, 20] and attenuated by obstacles (e.g. walls) (see Table III in [23]).

To overcome these challenges, state-of-the-art 60 GHz radios use high-gain, switched-beam directional antennas [21, 16]. High antenna gain helps increase

* Work done during internship at NEC Labs America, Inc.

the coverage range and overcome attenuation by obstacles while the ability to switch beams at run-time (i.e. beamsteering) can help steer signals “around” human-body blockage. A natural follow-up question is whether it is feasible to build *general-purpose, gigabit wireless LANs* using these state-of-the-art 60 GHz radios? Unlike existing use of this technology restricted to point-to-point, LOS scenarios [8, 17, 19], is it possible to extend its applicability to environments with NLOS blockage from walls/cubicles, human-body blockage, and user mobility?

Towards determining this feasibility, we measure 60 GHz link performance in an indoor enterprise environment. Through experiments in a realistic setting, this paper answers the following set of basic and important questions: *What is the effect of LOS or NLOS node location on performance? How sensitive is the performance to node (or more precisely, antenna array) orientation? How robust is the performance to human-body blockage and mobility?* To our knowledge, we are not aware of any other network-layer measurements that address all these generic questions in the indoor context. Prior efforts in this domain focused mainly on PHY-layer channel characterization [23, 3].

To conduct these measurements, due to the lack of availability of 60 GHz wireless interfaces for PCs, we build a first-of-its-kind experimental platform called *Presto*. *Presto* enables IP-over-60-GHz communication by leveraging commercial off-the-shelf (COTS) 60 GHz wireless HDMI radios and interfacing them with PCs via readily-available FPGAs.

In theory, high antenna gain can help overcome attenuation losses due to wall or cubicle blockage. Further, multipath reflections in indoor environments could present alternate paths that beamsteering can take advantage of in the presence of human-body blockage or while adapting to user mobility. We study how effective state-of-the-art 60 GHz radios are in dealing with these real-world situations. In particular, we make the following key observations: (1) 60 GHz radios are able to overcome NLOS blockage due to walls and cubicles; their coverage range is reduced relative to LOS scenarios but could still be enough to satisfy the needs of dense WLANs. (2) Antenna array orientation has a significant effect on performance even in the presence of indoor multipath reflections; mitigation strategies that add to the single antenna array at each node and dynamically select amongst them show potential to address this issue. (3) Finally, beamsteering is effective in dealing with low levels of human-body blockage and LOS mobility at walking speeds; existing implementations need to react faster in the presence of high levels of dynamically-occurring human-body blockage.

The rest of the paper is organized as follows. Background on state-of-the-art 60 GHz radios and beamsteering is presented in §2. Our experimental platform, *Presto*, is described in §3. §4 describes our experimental methodology and §5 presents our results and interpretations from our experiments. §6 concludes.

2 Background

Need for Directionality & Beamsteering: With omni-directional antennas, 60 GHz radios cannot support distances greater than a few meters (see Figure 1 in [4]). The millimeter(mm) wavelengths at these frequencies lead to reduced

antenna aperture areas, which in turn lead to much higher path loss [6] and susceptibility to blockage [20].

Fortunately, antenna directionality can be used to overcome these limitations since directionality is inversely proportional to the square of the wavelength (Chap. 15, [12]). The mm-wavelengths also enable antenna arrays with tens of elements on a single die thus promoting beamsteering [13, 14].

With the realization that directionality and beamsteering are essential, the WirelessHD [2] and WiGig [22] specifications, as well as the IEEE 802.11ad draft standard [9] for 60 GHz radios include the necessary mechanisms and protocol support at the MAC and PHY layers (see further details in Appendix in [10]).

Antenna Realization for Beamsteering: Typically, beamsteering is enabled by *switched-beam directional antennas* that provide a good trade-off among the available antenna technologies; they are less bulky than a collection of *fixed-beam antennas* [15] and simpler to implement and incorporate than *adaptive-beam antennas* [14]. A common way of realizing switched-beam antennas is by using *phased array antennas*. Phased array antennas consist of an array of antenna elements, the signals sent to which are weighted in both magnitude and phase. The applied weights help reinforce energy in a particular direction, thereby producing an antenna beam pattern with high Signal-to-Noise-Ratio (SNR) over an omni pattern in the desired direction contributing to a *directional/array gain*. *To realize beamsteering, several such beam patterns are generated with a phased array antenna such that they cover the entire azimuth (360°), and a specific beam pattern is dynamically chosen from the available set during run-time operation.*

Practical realizations in state-of-the-art 60 GHz radios use square or a rectangular array of elements in planar patch form [7]. These planar patch arrays are typically polarized in the horizontal or vertical direction (i.e. can steer beams in one of these directions), and have a limited angular range (< 180 degrees) [16, 21] over which beams can be steered. These characteristics raise questions as to how sensitive performance will be to real-world factors like relative node location, antenna array orientation, temporary blockage by human bodies and user mobility? These questions motivate our measurements in an indoor enterprise environment. Due to the unavailability of 60 GHz wireless interfaces for PCs, we first build a new experimental platform called Presto.

3 The Presto Platform

Presto currently contains two simplex 60 GHz links (see Figure 1(a)). The nodes hosting the 60 GHz transmitter (TX) and receiver (RX) are 2.8 GHz quad-core general-purpose PCs running Linux. The wireless TX and RX connect to the PCs through customized HDMI interface boards (HIB). Figure 1(b) shows a picture of the HIB, and Figure 1(c) shows the 60 GHz transceivers.

60 GHz Wireless Transceivers: We use the Vizio XWH200 wireless HDMI TX-RX pairs [21]. These TX-RX pairs can support a peak MAC throughput of 3Gbps (at the peak PHY rate of 3.8Gbps) and are based on Silicon Image, Inc.'s 2nd-generation WirelessHD 60 GHz radios [18] (see further details in Appendix in [10]). These devices are traditionally designed to support *uncompressed HD*

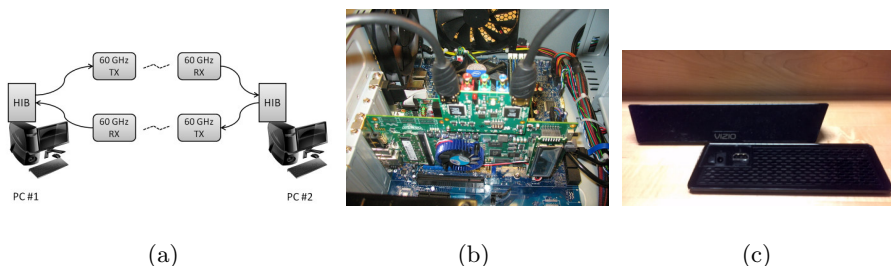


Fig. 1. The Presto Platform. (a) Setup Overview, (b) HIB on the PCIe interface on a quad-core PC, and (c) Vizio 60 GHz Transceivers.

video transfer from a Blue-ray player to an HDTV. While the 60 GHz MAC and PHY specifications have sufficiently matured [9, 2], the *protocol adaptation layer (PAL)* to interface the TCP/IP networking stack with 60 GHz transceivers is still under development [9, 2]. Consequently, only an HDMI interface is provided. Hence, our first challenge is to interface these transceivers with the PC to support IP-over-wireless-HDMI packet data communications.

HDMI-Interface Board (HIB): To enable IP-over-wireless-HDMI, we use a HDMI interface board (HIB) that interfaces with the PC over the PCIe bus. The HIB is an Altera Aria II GX FPGA development board [5] with Microtronix [11] HDMI transmitter and receiver daughter-cards. The HIB has two HDMI interfaces, one for transmit and one for receive. We consider two design options for the placement of the IP-to-HDMI conversion functionality on the FPGA: (a) placing full functionality in the FPGA, (b) splitting the functionality between the FPGA and the host processor.

In the first approach, the FPGA can hide all the complexity of IP-over-HDMI and expose an Ethernet interface to the networking stack. While this enables ease of experimentation, sufficient processing power and memory are needed on the FPGA in order to support multi-Gbps speeds, which can increase its cost significantly. In the second approach, the FPGA efficiently transfers raw data (in bytes) between the HDMI interface and the PC's RAM. The software on the host CPU can then interface with the RAM, create the abstraction of a network interface and implement data-link layer functionality (like framing). By offloading most of the functionality to the host PC, such an approach is cost-effective. But it needs fast CPUs to enable network processing at multi-Gbps speeds. Presto adopts the second approach to keep the FPGA simple and cost-effective, while relying on the ready availability of fast CPUs.

FPGA Logic: The software on the FPGA uses scatter-gather DMA (`sgdma`) logic to take data spread over memory and transfer it over PCIe to or from the Avalon memory-mapped bus on the FPGA. Additional logic transfers data between the Avalon bus and the HDMI transmit/receive ports. Such an approach enables high-speed transfers from RAM over PCIe to the HDMI ports.

To transfer binary IP traffic over the Vizio adapters, they are modified to use RGB mode to avoid data corruption due to color-space conversion (to YCrCb). This allows us to measure data corruption due to channel-induced errors alone.

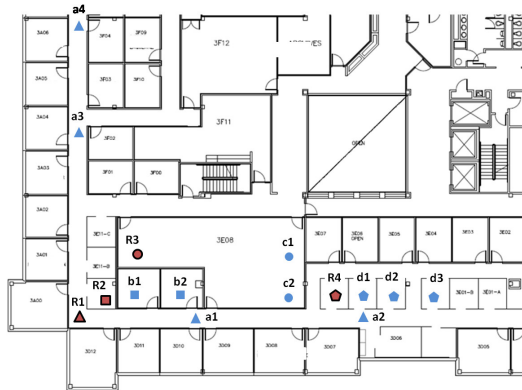


Fig. 2. Indoor Testbed; R1-R4: receivers, a1-d3: transmitters.

Among the RGB lines, we use the R-line to indicate that “valid” data from the PC is available on the G- and B-lines. This control-data split is needed since, HDMI video data, unlike IP traffic, is always flowing on the connection. *This split means that our current prototype can provide at most 2/3 of the raw capacity supported by these 60 GHz radios, i.e. 2/3 of 3 Gbps.* We plan to reduce this overhead in future versions of Presto.

Kernel-space Device Driver: To expose a byte-level file abstraction (primarily for ease and efficiency), the FPGA works in unison with a custom-built Linux device driver that hides the complexity of transferring data directly over the PCIe bus by exposing a standard POSIX API (i.e. open, read, write, close system calls). Once the driver is loaded, a `/dev/sgdma` device is created.

As a first case-study with Presto, we measure uni-directional (simplex), 60 GHz wireless link performance in an indoor enterprise environment.

4 Experimental Methodology

We conduct our measurements in a typical indoor enterprise environment with offices, cubicles, and corridors. Figure 2 shows our testbed deployed using Presto nodes. We consider four scenarios in eleven different TX, RX locations to capture different environmental effects, as summarized in Table 4(a).

To account for sensitivity to the TX/RX antenna array orientation, we divide the 360 degree X-Y plane into four orientations and vary them for each TX/RX location. This results in 16 TX/RX orientation combinations for each TX/RX location. We index each combination in Table 4(b) to ease our result description.

Traffic and Metrics: We generate backlogged traffic at 2 Gbps by using simple transmit and receive modules that directly write to and read from `/dev/sgdma` 32KB chunks of data in a loop for a specified amount of time³. Each experiment runs for 20 seconds and is repeated four times. We remove data from the start and end of experiments to avoid edge effects. We use *link goodput* as

³ We observe that when using lower than 32KB chunks, the PCs cannot fully utilize the available link capacity. Note that we use blocking reads and writes.

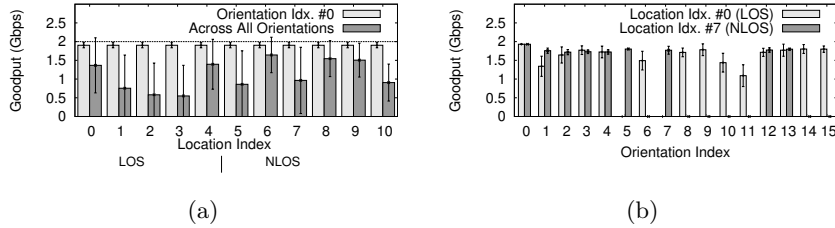


Fig. 3. 60 GHz link goodput at (a) all locations and (b) two specific locations.

the metric to quantify performance. Link goodput is measured as the average number of correctly received bits-per-second. Note that we account for both byte corruption (we send a known sequence of bytes) as well as loss.

5 Evaluation

In this section, we present several results that demonstrate in indoor environments: (a) the ability of 60 GHz radios to overcome wall/cubicle blockage, (b) their sensitivity to node (or antenna array) orientation, and (c) their robustness to human-body blockage and walking-speeds mobility (preliminary).

Effect of LOS/NLOS node location: For each of the eleven locations, Figure 3(a) shows the goodput when the nodes are aligned (i.e. Orientation Idx. #0) and across all X-Y orientations. When the nodes are aligned, goodput performance remains ~ 2 Gbps consistently irrespective of the LOS/NLOS nature of the location. *Thus, contrary to conventional perception, 60 GHz radios are able to overcome persistent blockage by walls and cubicles.* While the mean goodput does drop when we consider all orientations, it is still > 0.5 Gbps even in locations with persistent wall/cubicle blockage.

To investigate the high standard deviation in goodput across orientations, we plot the goodput for each orientation in two sample locations in Figure 3(b). A binary goodput behavior (i.e. either > 1 Gbps or zero) is revealed due to our use

Loc. Idx	Scenario	RX/TX	Distance	Blockage
0	Corridor	R1/a1	8m	LOS
1		R1/a2	20m	LOS
2		R1/a3	10m	LOS
3		R1/a4	25m	LOS
4	Lab	R3/c1	12m	LOS
5		R3/c2	12m	NLOS
6	Office	R2/b1	3m	NLOS (1 wall)
7		R2/b2	5m	NLOS (2 walls)
8	Cubicle	R4/d1	3m	NLOS (1 wall)
9		R4/d2	5m	NLOS (2 walls)
10		R4/d3	6m	NLOS (4 walls)

(a) Eleven TX/RX locations

Ori. Idx	RX	TX	Ori. Idx	RX	TX
0	→	←	8	←	←
1	→	↓	9	←	↓
2	→	→	10	←	→
3	→	↑	11	←	↑
4	↑	←	12	↓	←
5	↑	↓	13	↓	↓
6	↑	→	14	↓	→
7	↑	↑	15	↓	↑

(b) Sixteen TX/RX orientations

Fig. 4. Measurement location characteristics and TX/RX orientations tested.

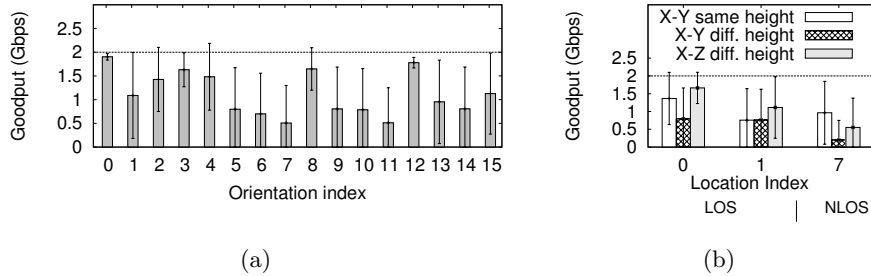


Fig. 5. Goodput (a) per-orientation across locations and (b) per-location across heights and orientations.

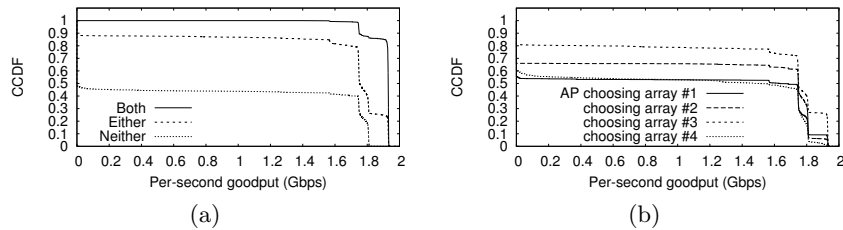


Fig. 6. Complementary CDF of (a) per-second link goodput across locations when both, either or neither side is aligned with the other, and (b) per-second link goodput when one side chooses from multiple fixed antenna arrays.

of a fixed PHY bit-rate. Overall, Figures 3(a) and 3(b) reveal that *performance is very sensitive to node orientation*. We study this effect in detail next.

Sensitivity to Node or Antenna Array Orientation: In real-world deployments, antenna array orientation on either TX/RX can be along any one of three dimensions. To account for this, we study the performance for different fixed orientations in the X-Y plane. We also consider the effect of relative height differences and orientations in the X-Z plane.

X-Y plane: Figure 5(a) shows for each TX/RX orientation, the mean and standard deviation in goodput across all locations. Mean goodput of all orientations is above 0.5 Gbps and 50% of the orientations have a goodput of above 1 Gbps. However, *performance of individual orientations varies widely across locations: standard deviation in goodput is > 0.5Gbps for a majority (14 out of 16) of orientations and the mean goodput between different orientations differs by up to 1.3 Gbps*. Thus, an orientation that works well in one location need not work well in another. This behavior is also visible in Figure 3(b): nine orientations (#5-11 and #14-15) provide > 1Gbps mean goodput in one location while providing zero goodput in the other location.

Different heights and the X-Z plane: In many real-world deployments (e.g. indoor enterprise WLANs), communicating entities are at different heights. Further, the antenna array can be oriented in the X-Z plane as well. This prompts us to place the TX and RX at different heights at three locations and measure the performance when the TX and RX antenna arrays are oriented in the X-Y and X-Z planes. In Figure 5(b), we compare these measurements with those when the TX and RX were at the same height, across orientations in the X-Y

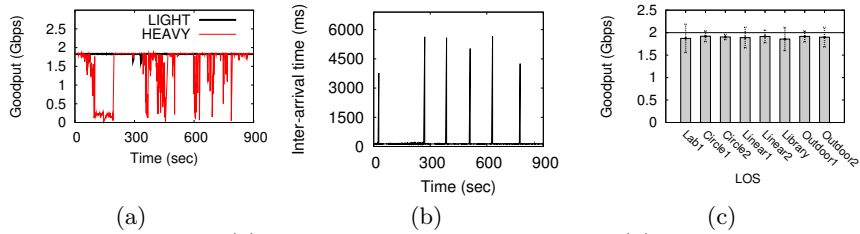


Fig. 7. Goodput with (a) light and heavy human activity. (b) Re-beamforming delay and (c) goodput with LOS mobility at walking-speeds.

plane. When the nodes are at different heights, mean goodput with X-Y plane orientation is much lower than that with X-Z orientation. In fact, even when the nodes are at the same height, for some locations (Idx. #0 and #1), this is the case. Thus, sensitivity to X-Z plane orientations should also be considered.

Importance of orienting towards the other side: To expand on the benefit of using orientation index #0 (see Figure 3), Figure 6(a) breaks down link goodput across all locations into when (a) both, (b) at least one, and (c) neither antenna array(s) are pointing towards the other side. Even when one antenna array is oriented towards the other side, goodput is greater than 1.5 Gbps 85% of the time with a median goodput of 1.7 Gbps. Further, when neither antenna array is aligned, goodput is 0 over 50% of the time!

Benefit of using multiple antenna arrays: One way of mitigating antenna array orientation mis-match is to use multiple antenna arrays at each node and dynamically selecting amongst them at run-time. Figure 6(b) shows the feasibility of such an approach by plotting the link goodput across all locations when one side (e.g. access point (AP)) chooses from amongst four antenna arrays corresponding to the four TX/RX orientations in the X-Y plane. Note that the other side (e.g. the client) can choose any orientation. *By choosing antenna array #3, the AP can recover a significant portion of performance loss due to antenna array orientation mis-match in the X-Y plane.*

Robustness to Human-body Blockage: We also design two experiments to study the behavior of 60 GHz transmissions in the presence of light and heavy human activity. The first experiment is conducted in a corridor with light human activity (occasional blockage by 1-2 human bodies). The second experiment is conducted during an informal tea-time gathering of people in a room (10m x 6m x 3m); on average 25-30 people were moving/standing in the room between the TX and the RX that were placed at two diagonally opposite corners of the room, oriented towards each other. The TX-RX channel is LOS in the absence of people. In each case, the transfer was done for 15 minutes and people were kept unaware of the experiments to avoid influencing the results. Goodput results for both experiments are shown in Figure 7(a)). *Beamsteering is quite robust to light human activity. With heavy human activity, while goodput fluctuates significantly in Figure 7(a), it is still high for long periods of time with a mean of 1.68Gbps.* When connectivity is lost, the transceivers perform re-beamforming and restart transfers. To measure the re-beamforming delay, we repeat the experiment in the absence of people but with explicit manual re-alignment of the receiver from

time to time. Figure 7(b) shows the re-beamforming delay for the current hardware implementation takes upto six seconds. Due to limited access to the 60Ghz transceivers at this level, we cannot completely justify the reason for such high delay to re-adjust the beam. However, we believe that the current implementation is primarily designed for static settings and that future implementations will react faster and reduce these delays significantly.

Robustness to Mobility (Preliminary): In Figure 7(c), we report goodput performance with walking mobility in nine locations (indoor and outdoor) with LOS between the TX and RX that have up to ~ 20 m distance between them. In each location, the RX moves at about 0.5 m/s, starting at the TX, and had LOS. In the “Circle1” and “Circle2” cases, TX-RX distance was ~ 5 m, and we do not see any negative effects of orientation mis-match. For simplicity, in all other cases the TX and RX were oriented towards each other. *Results indicate that 60 GHz radios can adapt to walking mobility with LOS.*

Implications for Next-Generation Gigabit WLANs: Presto currently uses 60 GHz radios from one manufacturer restricting our evaluation to a single implementation of beamsteering and PHY-layer configuration. This is primarily due to the unavailability of COTS 60 GHz radios from other manufacturers. However, our preliminary experiments reveal a LOS range of 25m and NLOS range of ~ 6 m in an indoor enterprise setting. Since the current implementation uses the highest PHY bit-rate, we anticipate that both ranges should improve via the use of lower bit-rates (via more robust modulation and coding). Taken together with the rest of our results, 60Ghz radios show strong potential for use in either (a) high-density gigabit WLANs (where APs are placed tens of meters apart) and/or (b) WLANs in conjunction with Wifi to increase capacity.

Moreover, since Presto is designed to work with any 60 GHz wireless HDMI radio, it can be used to measure performance for radios from multiple vendors once they are available, and we expect to see similar results. This work opens up interesting and challenging questions for future work: (a) what about adaptation to mobility and human-body blockage in light of sensitivity to orientation?, (b) how well can these radios deal with co-channel interference? (c) while MAC scheduling [22, 9] may mitigate deafness concerns in single-cell WLANs, what about coordinated/uncoordinated multi-cell networks?

6 Conclusion

In this paper, we study the link-level performance of state-of-the-art 60 GHz radios in the context of robustness to blockage by walls, cubicles, and human-bodies, adaptation to walking-speeds mobility, as well as sensitivity to antenna array orientation. We make the following key observations: (1) 60 GHz radios are able to overcome NLOS blockage due to walls and cubicles; their coverage range is reduced relative to LOS scenarios but could still be enough to satisfy the needs of dense WLANs. (2) Antenna array orientation has a significant effect on performance even in the presence of indoor multipath reflections; mitigation strategies that add to the single antenna array at each node and dynamically select amongst them show potential to address this issue. (3) Finally, beamsteering

is effective in adapting to low levels of human-body blockage and LOS mobility at walking speeds; existing implementations need to react faster in the presence of high levels of dynamically-occurring human-body blockage.

References

1. MAC and PHY Specifications for High Rate WPANs, mm-wave-based alternative PHY extension. *IEEE Std 802.15.3c-2009 (Amendment to IEEE Std 802.15.3-2003)*, pages 1–187, Oct. 2009.
2. WirelessHD Specs. <http://tinyurl.com/2ehkq6f>, August 2009.
3. S. Collonge, G. Zaharia, and G. Zein. Influence of the Human Activity on Wideband Characteristics of the 60 GHz Indoor Radio Channel. *IEEE Trans. on Wireless Commun.*, 3(6):2396–2406, Nov. 2004.
4. C. Cordiero. Evaluation of Medium Access Technologies for Next Generation Millimeter-Wave WLAN and WPAN. In *ICC*, 2009.
5. A. Corp. Arria II GX FPGA Development Kit. <http://www.altera.com/products/devkits/altera/kit-aiigx-pcie.html>.
6. C. Doan and et. al. Design considerations for 60 GHz CMOS radios. *IEEE Communications Magazine*, 42(12):132–140, Dec. 2004.
7. J. Gao, K. Li, T. Sato, J. Wang, H. Harada, and S. Kato. Implementation considerations of patch antenna array for 60 GHz beam steering system applications. In *Radio and Wireless Symposium*, pages 31–34, San Diego, CA, USA, 2009.
8. D. Halperin, S. Kandula, J. Padhye, P. Bahl, and D. Wetherall. Augmenting data center networks with multi-gigabit wireless links. In *ACM SIGCOMM*, 2011.
9. IEEE TGad. PHY/MAC Complete Proposal Spec. (approved as D0.1). <http://tinyurl.com/2fqkxx>, May 2010.
10. K. Ramachandran et. al. On 60 GHz Wireless Link Performance in Indoor Environments. <http://www.nec-labs.com/~rajesh/60G.pdf>, 2011. NECLA TR.
11. Microtronix Datacom. HDMI Receiver, Transmitter HSMC daughter card. <http://tinyurl.com/4re97a5>, 2011.
12. S. Orfanidis. *Electromagnetic Waves and Antennas*. Rutgers University, 2008.
13. M. Park and P. Gopalakrishnan. Analysis on spatial reuse and interference in 60-ghz wireless networks. *IEEE J.Sel. A. Commun.*, 27:1443–1452, October 2009.
14. K. Ramachandran and et. al. Adaptive Beamforming for 60 GHz Radios: Challenges and Preliminary Solutions. In *ACM mmCom*, pages 33–38, 2010.
15. K. Ramachandran and et. al. On the Potential of Fixed-beam 60 GHz Network Interfaces in Mobile Devices. In *PAM*, pages 62–71, 2011.
16. Rocketfish, Inc. Rocketfish - WirelessHD Adapter. <http://tinyurl.com/4pdzqac>.
17. SiBeam. OmniLink60. <http://www.sibeam.com/>, 2010.
18. SiBeam. SB9220/SB9210 WirelessHD Chip. <http://tinyurl.com/2535v8u>, 2010.
19. S. Singh, R. Mudumbai, and U. Madhow. Interference analysis for highly directional 60-ghz mesh networks: The case for rethinking medium access control. *Networking, IEEE/ACM Transactions on*, PP(99):1, 2011.
20. S. Singh, F. Ziliotto, U. Madhow, E. M. Belding, and M. Rodwell. Blockage and Directivity in 60 GHz Wireless PANs. *IEEE JSAC*, 27(8):1400–1413, 2009.
21. Vizio, Inc. Universal Wireless HD Video and Audio Kit (XWH200). <http://www.vizio.com/accessories/xwh200.html>.
22. WiGig Alliance. WiGig Specs. <http://tinyurl.com/29sql4q>, May 2010.
23. H. Xu, V. Kukshya, and T. Rappaport. Spatial and Temporal Characteristics of 60 GHz Indoor Channels. *IEEE JSAC*, 20(3):620–630, 2002.